ACS APPLIED MATERIALS & INTERFACES

Research Article

Cite This: ACS Appl. Mater. Interfaces 2019, 11, 46472−46478

www.acsami.org

Paper-Based Radial Chromatographic Immunoassay for the Detection of Pathogenic Bacteria in Milk

Ke Luo, Jian Ryu, In-Hye Seol, Ki-Baek Jeong, Sang-Mook You, and Young-Rok Kim*

Graduate School of Biotechnology & Department of Food Science and Biotechnology, Kyung Hee University, Yongin 17104, Korea

Supporting Information

ABSTRACT: Here, a paper-based radial flow chromatographic immunoassay (RFCI) employing gold nanoparticles (AuNPs) as chromatic agents was developed for the detection of *Escherichia coli* O157:H7 in whole milk. A 4-repeated gold-binding peptide-tagged (4GBP) streptococcal protein G (SPG) fusion protein was constructed as a bifunctional linker to immobilize antibodies on the surface of AuNPs with a well-oriented form based on the specific affinity of GBP and SPG to the gold and Fc portion of the antibody, respectively. 4GS@AuNPs prepared with the bifunctional linker protein exhibited excellent colloidal stability even at high salt concentrations of up to 500 mM, which is a critical requirement for its application to a broad range of biological and food samples. The enhanced colloidal stability and excellent binding capability of the immuno-4GS@AuNPs toward target bacteria lowered the detection limit of RFCI for target pathogenic bacteria in whole milk as low as 10^3 CFU/mL, which is by an order of magnitude lower than that of conventional immuno-AuNPs prepared with physical adsorption of antibodies. The RFCI pattern could also be converted into a grayscale value by simple image processing for quantitative determination of target pathogenic bacteria. This paper-based detection system would provide an effective means of monitoring the presence of food-borne pathogens in real food samples with naked eyes.

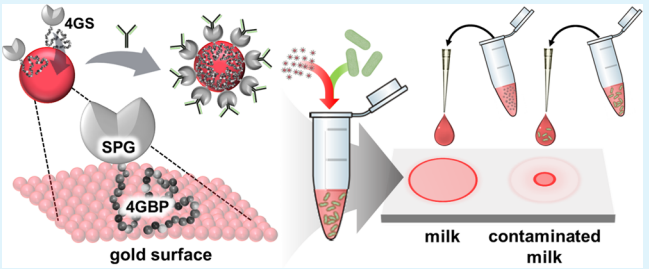

KEYWORDS: *radial chromatography, gold nanoparticles, biosensor, fusion protein, immunoassay, conjugation*

INTRODUCTION

Foodborne illness caused by pathogenic microorganisms is one of the most serious threats to human health, and early diagnosis of bacterial contamination is thus critical to ensure the safety of food and appropriate treatment.[1,2] Paper-based colorimetric sensors employing antibody-conjugated gold nanoparticles (immuno-AuNPs) have become a powerful and versatile toolbox for the specific detection of biomarkers in various bioanalytical systems. With their advantages over the conventional approaches (e.g., plate counting, PCR, ELISA, etc.), paper-based colorimetric sensors, such as lateral flow assay (LFA), have great potential as a point-of-care diagnostics platform that can instantly identify the presence of pathogenic microorganisms in food samples.[3,4] However, the sensitivity of LFA for the detection of intact bacteria is typically over 10^5 CFU/mL, which does not meet the requirements of most regulatory standards for ensuring the safety of food.[1] The intensity of the colorimetric signal in LFA is proportional to the molar concentration of the target analyte in the sample and the number of chromatic labels attached to the single target molecule. The typical LFAs with a detection limit of nanomole or picomole are capable of detecting 10^8 to 10^{11} target particles or molecules, which is not sensitive enough for bacterial detection. Thus, there have been enormous efforts to improve the sensitivity of LFA for the detection of microorganisms through signal amplification and pre-enrichment steps. For example, nucleic acid-based LFA can provide an effective means of detecting target bacteria because the nucleic acids, such as RNA or DNA, are small biomolecules that readily flow through the membrane of test strips, and the sensitivity of LFA could be improved by employing PCR to amplify the number of target nucleic acids that are subsequently analyzed by LFA.[5] The use of chromatic nanoparticles in combination with enzyme, such as horseradish peroxidase, could also improve the sensitivity of LFA by 1 or 2 orders of magnitude.[6] However, these methods require a multistep procedure, such as pre-enrichment, nucleic acid extraction, amplification, or color development by chromatic substrates, which limit its on-site applications.[7]

In addition, well-oriented immobilization of antibody on the surface of chromatic agents, such as gold nanoparticles (AuNPs), as well as ensuring the colloidal stability of the chromatic immuno nanoparticles are highly desirable because the chromatic nanoparticles with antibodies in random orientation and aggregation form could result in poor capture efficiency, thus lowering the performance of LFA. A number of methods have been developed and applied for immobilization of antibodies to the surface of chromatic nanoparticles.[8] Conjugation of antibodies on the surface of AuNPs through covalent cross-linking (e.g., EDC-NHS chemistry) and physical

Received: September 5, 2019
Accepted: November 20, 2019
Published: November 20, 2019

DOI: 10.1021/acsami.9b16075
ACS Appl. Mater. Interfaces 2019, 11, 46472−46478

adsorption (e.g., pH-mediated adsorption) are the most commonly used methods. In particular, pH-mediated physical adsorption is based on ionic and hydrophobic interactions between the antibodies and AuNPs when pH is maintained around their isoelectric point.[9] However, this method has several drawbacks, including relatively high loss of antibodies during the immobilization process and randomly oriented adsorption of antibodies, which could deteriorate the binding efficiency of the chromatic agent toward target analytes.[10] In addition, the antibodies adsorbed on AuNPs surface can be exchanged by other molecules in the reaction sample because the conjugation is based on noncovalent adsorption. On the other hand, immobilization of antibodies on the surface of AuNPs through bifunctional fusion proteins that consist essentially of an immunoglobulin-binding domain (e.g., protein G) and a protein having a high affinity to gold surface (e.g., gold-binding peptide, GBP) would provide an effective means of immobilizing antibodies to the surface of gold nanoparticles in a well-oriented form, while keeping the antibodies in a biologically active conformation.[11−14] Cysteine-tagged protein G was also employed for the oriented immobilization of antibodies onto the gold chip.[15] In this case, the affinity of the thiol group in cysteine to gold surface was the basis of immobilization. However, there are more factors that need to be taken into account when immobilizing linker proteins or antibodies on the surface of colloidal gold in comparison to those on the surface of a gold chip. When applied to a sensing system, the colloidal golds with ligands on the surface are typically subjected to a range of physical and chemical agitation induced by centrifugation and unfavorable salt concentration and pH, which could bring about undesirable aggregation of the colloidal golds. Therefore, there is a need to develop an effective way of preparing stable immuno-AuNPs that could maintain their colloidal stability even under a harsh environment. Here, we present a paper-based radial flow chromatographic immunoassay (RFCI) using AuNPs as the chromatic agents for the rapid and sensitive detection of *Escherichia coli* O157:H7 (Scheme 1). Immuno-AuNPs were prepared by using a genetically engineered quadruply repeated GBP-tagged staphylococcal protein G (4GS) fusion protein as the bifunctional bioligand, which not only enabled the oriented immobilization of antibodies onto AuNPs but also improved the colloidal stability of the nanoparticles in aqueous solution even in the presence of high concentrations of salt. The performance of conventional LFA for bacterial detection is limited by the low mobility of the microorganism toward the detection zone through the nitrocellulose membrane (NCM), resulting in lengthy running time and low sensitivity. In this study, we exploited the size-dependent mobility of the analytes and chromatic agent in radial form upon application of a drop of the sample solution onto the NCM. The low mobility of target bacteria labeled with chromatic immuno-AuNPs resulted in the formation of an inner ring, whose intensity is proportional to the concentration of target bacteria. In the absence of target bacteria, all chromatic immuno-AuNPs evenly diffuse out in the radial direction without the formation of the inner ring. The enhanced binding capacity and excellent colloidal stability of the immuno-AuNPs achieved by the bifunctional ligand, 4GS, are investigated along with its practical application in detecting target bacteria in real food samples.

Scheme 1. Schematic Illustration of Paper-Based RFCI[a]

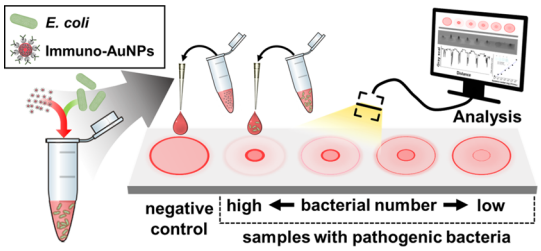

[a]The size-dependent differential mobility of the target analyte and chromatic agent (immuno-AuNPs) is the key for the detection system. The RFCI pattern can be converted to a grayscale value by simple image processing.

EXPERIMENTAL SECTION

Preparation and Characterization of 4GS@AuNPs. AuNPs were synthesized as reported by Kumar, et al. with a slight modification.[9] In brief, 1 mL of 12.7 mM $HAuCl_4$ solution was mixed with 49 mL of deionized water in a clean 100 mL glass flask with a magnetic stir bar, and the flask was sealed with aluminum foil. The mixture in the flask was heated to boil on a heating mantel with vigorous stirring. When the mixture started to boil, 0.94 mL of 38.8 mM trisodium citrate was added to the reaction. After the color changed from yellow to ruby red, the solution was subjected to a gentle boiling for another 10 min and cooled down to room temperature. The 1GS or 4GS linker protein was added to 1 mL of the synthesized AuNPs solution ($OD_{520} \approx 1.5$) to a final concentration of 50 μg/mL. The mixture was gently rotated at RT for 1 h, and then washed with 20 mM HEPES buffer (pH 7.5) three times by centrifugation at 7000*g* for 30 min, and the excess protein was transferred to a fresh EP tube. The amount of immobilized linker peptides, 1GS and 4GS, on the surface of the AuNPs was measured by subtracting the amount of unbound proteins after the binding reaction from the total amount that we used for the binding test. Coomassie Plus (Bradford) assay reagent (20 μL, Pierce; Thermo Fisher Scientific, Rockford, IL, USA) was mixed with 180 μL of the supernatants obtained by the centrifugation of the binding reactions. After 10 min of incubation, the absorbance was measured at 595 nm using UV−vis spectrophotometer (Infinite 200 PRO, TECAN, Switzerland). Bovine serum albumin (BSA) with a concentration ranging from 10 to 150 mg/mL was used as the control for the quantification.

Colloidal Stability of AuNPs. The colloidal stability of pristine AuNPs, 1GS@AuNPs, and 4GS@AuNPs was tested in salt solution containing varying concentrations of NaCl ranging from 125 to 500 mM. The absorption spectra of pristine AuNPs, 1GS@AuNPs, and 4GS@AuNPs in the presence of varying concentrations of NaCl (0−500 mM) were analyzed by the UV−vis spectrophotometer (TECAN) at wavelengths ranging from 400 to 800 nm. The morphology and surface composition of pristine AuNPs and 4GS@AuNPs were characterized by using field emission transmission electron microscopy (TEM, JEM-2100F, JEOL, USA) and an X-ray photoelectron spectroscopy (XPS, Theta Probe, Thermo Fisher Scientific, USA), respectively.

Preparation of Immuno-AuNPs. The synthesized AuNPs and 4GS@AuNPs were treated with anti-*E. coli* O157 monoclonal antibody to prepare antibody-functionalized gold nanoparticles, which were named immuno-AuNPs and immuno-4GS@AuNPs, respectively. In brief, 4 μg of anti-*E. coli* O157 antibody was added to the solution containing 4GS@AuNPs ($OD_{520} \approx 1.5$) and incubated at RT for 30 min with a gentle rotation. The conjugation solution was then centrifuged at 7000*g* for 30 min, and the supernatant containing unbound antibodies was discarded. The pellet was resuspended in phosphate-buffered saline (PBS, pH 7.4) containing 0.3% (w/v) BSA and 0.01% (v/v) Tween-20 and stored in a dark bottle at 4 °C until use. The binding of the antibody to colloidal pristine AuNPs by

DOI: 10.1021/acsami.9b16075
ACS Appl. Mater. Interfaces 2019, 11, 46472−46478

physical adsorption depends on the pH of the binding solution. The optimal pH for the binding of anti-*E. coli* O157 monoclonal antibody to AuNPs was determined to be 7.5. Thus, the pH of pristine AuNPs solution and antibody was adjusted to pH 7.5 with 0.1 N NaOH. Anti-*E. coli* O157 monoclonal antibody (4 μg) was added to 200 μL of 20 mM HEPES (pH 7.5) containing pristine AuNPs ($OD_{520} \approx 1.5$). The resulting immuno-AuNPs were washed and stored as described above. The number of immobilized antibodies to pristine AuNPs and 4GS@AuNPs was determined by the Bradford assay as aforementioned.

Detection of Target Bacteria by RFCI. Freshly cultured *E. coli* O157:H7 was washed three times with PBS and diluted serially to the concentrations ranging from 10^0 to 10^5 CFU/mL in PBS or sterilized whole milk. The number of bacteria in the test solution was confirmed by plate counting method, in which the 0.1 mL of the serially diluted cell suspensions was plated on Luria broth agar plates (1% tryptone, 0.5% yeast extract, 1.0% NaCl, and 2.0% agar, w/v; pH 7.2), and incubated at 37 °C for 24 h. The number of bacteria in the original test solution was calculated by multiplying the number of colonies on each plate by the dilution factors. For RFCI, 1 mL of the sample was centrifuged at 5000*g* for 5 min, and 0.9 mL of the supernatant was discarded. After gentle mixing, 90 μL out of the remaining 0.1 mL pellet solution was transferred to a new tube and mixed with 10 μL of the immuno-4GS@AuNPs ($OD_{520} \approx 3.0$) solution, followed by incubation at RT for 5 min. A 10 μL aliquot of the reaction mixture was applied onto the NCM, letting the solution radially diffuse outward. The resulting NCM with a characteristic diffusion pattern was imaged by using a scanner (HP OfficeJet 8660, Hewlett-Packard, Palo Alto, CA, USA), which was subsequently analyzed with the ImageJ NIH image processing software (Bethesda, MD). The intensity of the diffusion pattern on the NCM was measured in grayscale value (G). The signal intensity was determined by the ratio of the inner ring (G_I) over the total grayscale (G_T) as shown below

$$\Delta G = (1 - G_I/G_T) \times 100 \quad (1)$$

The presence of immuno-4GS@AuNPs on the surface of *E. coli* O157:H7 was analyzed by transmission light microscopy (TLS, Nikon TE2000U, Tokyo, Japan) and scanning electron microscopy (SEM, TM 3000, Hitachi, Tokyo, Japan). The presence of *E. coli* O157:H7 within the matrix of the NCM was investigated by using high-resolution SEM (MERLIN Carl Zeiss, Oberkochen, Germany).

RESULTS AND DISCUSSION

In this study, we employed the 4-repeated gold binding peptide-tagged protein G (4GS) fusion protein as an effective bifunctional linker to immobilize an antibody to the surface of gold nanoparticles (AuNPs) (Figure 1a). Considering that the affinity of GBP to gold surface is originated from the close contact of the polar and cationic side chains to the underlying gold lattice,[16,17] amino acid sequence of GBP that was tagged to the streptococcal protein G (SPG) domain was repeated four times in order to enhance its binding affinity to the gold surface (Figure S1). The constructed expression vector, pET-21a(+):*histag/4gbp-spg*, encoding 4GS linker protein was transferred to *E. coli* BL21 (DE3) for over expression. The protein was purified by using a Ni-NTA affinity column, and the molecular size of the protein was determined to be 27.84 kDa (Figure S2). On the other hand, uniform-sized AuNPs were prepared by the classical citrate synthesis method.[9] The UV−vis spectra of the synthesized AuNPs exhibited a characteristic surface plasmon resonance (SPR) band at 520 nm and the corresponding red color. Upon addition of 4GS fusion protein to the AuNPs solution, the SPR band was red-shifted by 3 nm without increasing the intensity of the shoulder band, suggesting the adsorption of 4GS fusion proteins onto the surface of AuNPs without aggregation of the functionalized gold nanoparticles (Figure 1b). TEM images of

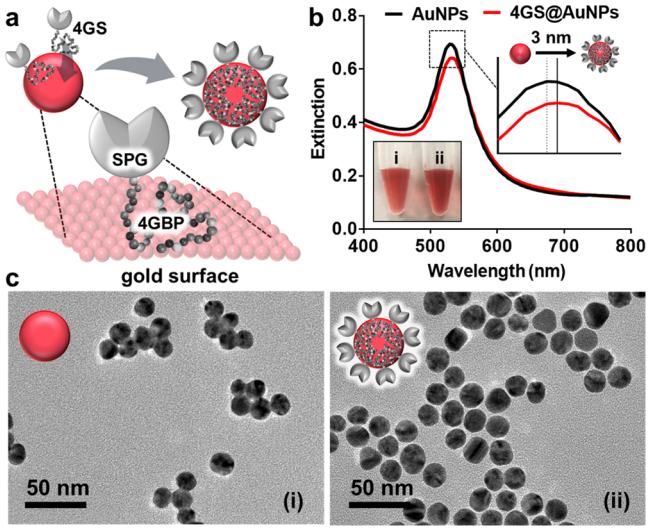

Figure 1. (a) Schematic illustration showing the bioconjugation of 4GS fusion proteins to the surface of AuNPs. (b) UV−vis spectra of pristine AuNPs and 4GS@AuNPs. The inset at the lower left corner shows photographs of the corresponding solution of AuNPs before (i) and after (ii) treatment with 4GS fusion proteins. The inset at the upper right corner shows the magnified view of the UV−vis absorbance peaks, indicating a 3 nm red-shift of the SPR band of AuNPs when conjugated with 4GS fusion proteins. (c) TEM image of pristine AuNPs (i) and 4GS@AuNPs (ii).

the pristine AuNPs showed spherical nanoparticles with a mean particle diameter of ~20 nm (Figures 1c and S3). The pristine AuNPs were shown as an aggregated form probably due to the drying process before TEM analysis. On the other hand, the AuNPs coated with 4GS fusion proteins clearly showed a gap between particles due to the presence of the linker protein on the surface, preventing the aggregation of AuNPs (Figure 1c). In addition, the adsorption of 4GS fusion proteins caused a decrease in the negative surface charge density of AuNPs (Figure S4), implying that the adsorbed peptides might confer the steric stabilization of AuNPs to prevent particle aggregation during the drying process.[18]

We found that the presence of 4GS fusion proteins on the surface of AuNPs (4GS@AuNPs) enhanced the colloidal stability of AuNPs even in the presence of a high concentration of NaCl (500 mM) (Figure 2). It is worth noting that both pristine AuNPs and AuNPs coated with SPG or 1GS fusion protein (SPG@AuNPs or 1GS@AuNPs) were sensitive to the presence of salt, NaCl, even at low concentration (125 mM) (Figure 2a−c), resulting in the aggregation of the gold nanoparticles and loss of the characteristic SPR peak. The strong affinity of 4-repeated GBP to the surface of AuNPs prevented the diffusion of the linker protein from the nanoparticles and subsequent aggregation of AuNPs in aqueous solution even at high salt concentration. The higher affinity of the 4GS linker protein to the surface of gold was evidenced by its binding test. When treated with the same concentration of AuNPs, the amount of 4GS bound to the AuNPs was about 2-fold greater than that of 1GS (Figure S5), suggesting that the affinity of the linker protein to gold surface could be enhanced by increasing the repeating unit of GBP to 4×. The colloidal stability of AuNPs is particularly important when applied to the paper-based capillary flow chromatography. Upon application onto the NCM, pristine AuNPs were readily diffused out in radial form along with water by capillary

DOI: 10.1021/acsami.9b16075
ACS Appl. Mater. Interfaces 2019, 11, 46472−46478

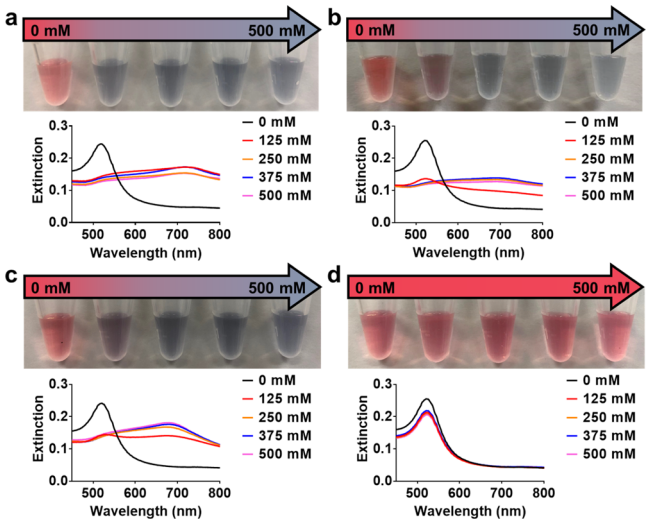

Figure 2. Colloidal stability of (a) pristine AuNPs, (b) SPG@AuNPs, (c) 1GS@AuNPs, and (d) 4GS@AuNPs at varying concentrations of NaCl from 0 to 500 mM. Pink solution represents well dispersed and stable suspension of AuNPs. UV−vis spectra of the corresponding samples are shown below.

action (Figure S6). However, the mobility of AuNPs was dramatically decreased in the presence of salt (100 mM NaCl), leading to the formation of a small dark purple inner ring deposit (Figure S6). Such a problem associated with the colloidal instability of AuNPs in the presence of salt was successfully resolved by introducing 4GS as a bifunctional linker protein to the surface of gold nanoparticles.

The presence of bifunctional linker protein on the surface of AuNPs was confirmed by XPS. XPS analysis of the Au 4f and S 1s were not included in this study because the adsorption of the peptides was not mediated through Au−thiol linkages.[16,17] The XPS spectra of the 4GS@AuNPs showed the characteristic peaks for C 1s, N 1s, and O 1s, where the presence of N 1s indicated the adsorption of peptides on the gold surface (Figure 3). The O 1s peak that represents the surface oxidation state of AuNPs was clearly diminished in 4GS@AuNPs in comparison to that in pristine AuNPs possibly due to the close contact of the polar amino acids (e.g., serine and threonine) in alignment with the underlying gold lattice.[16] The C 1s core level spectrum of pristine AuNPs exhibited three main components which are originated from C−C at ∼283.8 eV,

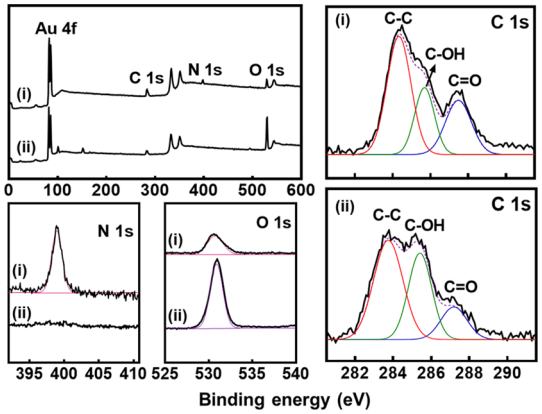

Figure 3. XPS survey scan of 4GS@AuNPs (i) and pristine AuNPs (ii) with individual high resolution XPS spectra of N 1s, O 1s, C 1s.

C−OH at ∼285.2 eV, and C═O at ∼287.2 eV due to the presence of citrate on the surface of AuNPs.[19] On the other hand, the intensity of the C−OH peak was diminished, whereas the intensity of the C−C bond remained dominant when the AuNPs were coated with 4GS. The results clearly support that the linker protein is stably immobilized onto the surface of AuNPs by physisorption.

To investigate the anchoring effect of the bifunctional linker for oriented immobilization of the antibody, the number of antibodies immobilized on the gold nanoparticles via 4GS fusion protein was measured in comparison to that immobilized via pH-mediated adsorption. As shown in Figure 4a, pristine AuNPs exhibited a higher saturation concentration of immobilized antibodies when compared to that of 4GS@AuNPs. The higher concentration of antibodies on the surface of pristine AuNPs might be attributed to the adsorption of the antibodies with random orientation, which could lead to the aggregation or partial denaturation of antibodies on the gold surface. This could negatively affect the affinity or accessibility of the immuno-AuNPs for target bacteria due to the steric hindrance induced by improper orientation of the antibody sideways or downward to the surface of AuNPs.[20] The low saturation concentration of antibodies on the surface of 4GS@AuNPs would suggest the fact that the nonspecific adsorption of antibodies to the surface of AuNPs is prevented by the bifunctional linker protein and the antibodies immobilized through the linker protein are oriented in the right conformation.

TLS and SEM analysis were performed to confirm the specific binding of the resulting immuno-4GS@AuNPs to the target bacteria, *E. coli* O157:H7, through antigen−antibody interaction. TLS clearly showed that the surface of *E. coli* O157:H7 was densely coated with immuno-4GS@AuNPs (Figure 4b). Under TLS, the target bacteria were shown in black, indicating full coverage of the bacteria with immuno-4GS@AuNPs that blocked the transmission of light through the bacteria. As shown in the inset of Figure 4b, the bacteria without immuno-4GS@AuNPs were almost transparent to the incoming light. SEM analysis also showed the presence of large number of immuno-AuNPs on the surface of bacteria, which is shown as brightly scattered spots (Figure 4c). These results demonstrate that the 4GS fusion protein could serve as an effective anchoring adaptor for the immobilization of antibodies in the oriented form onto the surface of AuNPs along with significantly enhanced colloidal stability.

The radial diffusion characteristics of immuno-4GS@AuNPs in the presence or absence of *E. coli* O157:H7 on the NCM were investigated (Figure 5a). The principle of the assay is the size-dependent differential mobility of the target analyte and chromatic immuno-AuNPs through the NCM. As shown in Figure 5b, immuno-AuNPs that were coupled with the anti-*E. coli* O157 monoclonal antibody underwent outward flow in a radial form by capillary action, leading to the formation of a ring-like deposit at the edge with the typical red color of the AuNPs (Figure 5b). When target bacteria were present in the sample, the chromatic immuno-AuNPs are specifically bound to the target bacteria, *E. coli* O157:H7, and formed a red ring-shaped deposit (Figure 5b). The diameter of the red ring deposit is equivalent to the droplet size of the sample solution, implying that the mobility of the target bacteria labeled with the immuno-4GS@AuNPs is restricted to the drop zone, whereas nonbound immuno-4GS@AuNPs are freely diffusing outward by the capillary action of water through the NCM.

DOI: 10.1021/acsami.9b16075
ACS Appl. Mater. Interfaces 2019, 11, 46472−46478

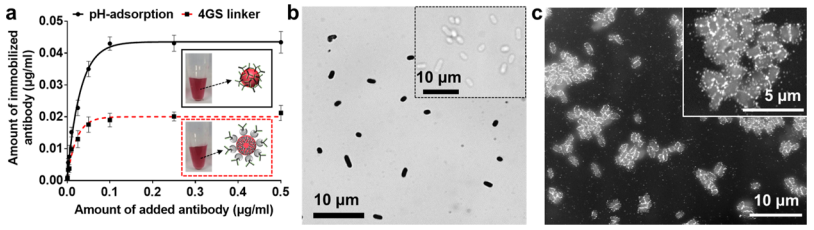

Figure 4. Immobilization of antibodies on the surface of AuNPs through pH-mediated adsorption and 4GS fusion proteins. (a) Amount of antibodies on the surface of AuNPs immobilized by the pH-mediated method (solid line) and the bifunctional protein (dashed line) as a function of the antibody concentration in the immobilization reaction. The inset shows the reaction tubes containing AuNPs (upper) and 4GS@AuNPs (lower) treated with 0.1 μg/mL of antibody. (b) TLS and (c) SEM image of *E. coli* O157:H7 labeled with anti-*E. coli* O157 immuno-4GS@AuNPs, in which the antibody was immobilized through 4GS linker proteins. The inset in the TLS image (b) show *E. coli* O157:H7 in the absence of immuno-4GS@AuNPs. The bright dots in the SEM image represent immobilized immuno-4GS@AuNPs on the surface of bacteria. Magnified SEM image of the bacteria labeled with immuno-4GS@AuNP is shown in the inset.

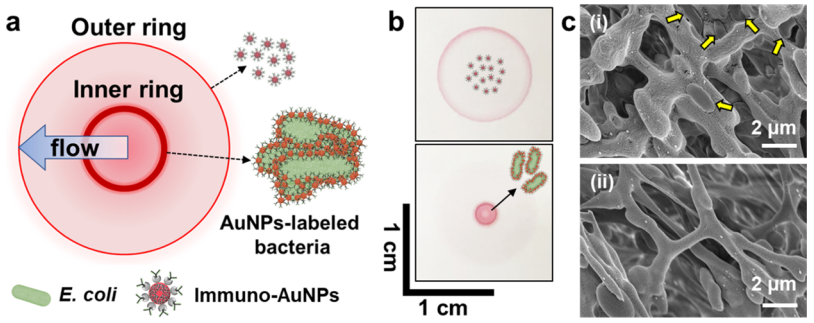

Figure 5. (a) Schematic illustration of paper-based RFCI for the detection of *E. coli* O157:H7 using immnuo-4GS@AuNPs. The target bacteria labeled with the immuno-4GS@AuNPs are trapped within the inner circle, whereas nonbound immuno-4GS@AuNPs are diffusing further in a radial form together with water. The red color in the RFCI pattern is derived from the chromatic immuno-4GS@AuNPs. (b) Photograph of the RFCI pattern generated from the sample without (upper) and with (lower) target bacteria. (c) SEM images of the matrix of NCM inside (i) and outside (ii) of the inner ring after application of the sample solution containing target bacteria. The bacteria (yellow arrows) are only present within the inner ring of the RFCI pattern in the NCM.

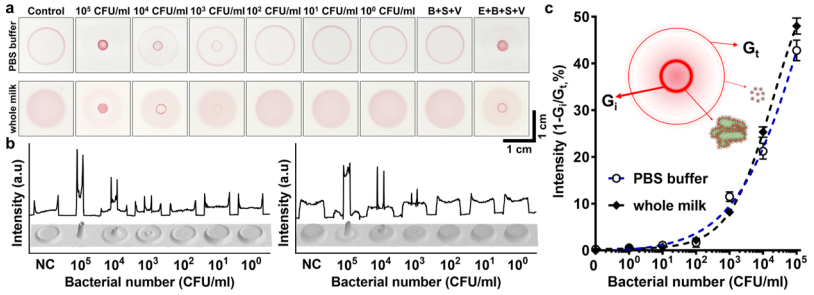

Figure 6. (a) RFCI patterns obtained from the samples containing varying concentrations of *E. coli* O157:H7 in PBS buffer (upper) and whole milk (lower) using immuno-4GS@AuNPs. *Bacillus cereus* (B), *Staphylococcus aureus* (S), and *Vibrio cholerae* (V) were employed as nontarget controls. (b) Grayscale analysis of the RFCI pattern generated from the sample with varying concentrations of *E. coli* O157:H7 in PBS buffer (left) and whole milk (right) using ImageJ software. (c) Plot showing the intensity of grayscale value vs bacterial concentration in PBS buffer (hollow circle) and whole milk (filled square). The intensity of signal was determined by the ratio of the grayscale value observed within the inner ring (G_I) to the total grayscale value (G_T) in the RFCI pattern.

Furthermore, the distribution of target bacteria on the NCM was investigated by SEM analysis. The SEM images showed that a number of rod-shaped *E. coli* O157:H7 were only observed within the inner ring on the NCM (Figure 5c), indicating that the size of *E. coli* O157:H7 is too large to travel through the dense matrix of the membrane. From the results, it is clear that nonbound immuno-4GS@AuNPs freely diffuse all the way out to the edge of the radial flow that forms a red outer ring pattern, whereas the immuno-4GS@AuNPs bound to the surface of target bacteria remain on the drop site because the bacteria is too large to travel through the dense matrix of the NCM, forming a red inner ring.

The ability of RFCI to detect *E. coli* O157:H7 was evaluated using a sample containing various numbers of bacteria from 10^0 to 10^5 CFU/mL. As shown in Figure 6a, the immuno-4GS@AuNPs were radially diffused out from the drop zone by the capillary action of the liquid in porous NCM for the negative control (a sample without *E. coli* O157:H7). On the other hand, the presence of target bacteria, *E. coli* O157:H7, resulted in the formation of a red inner ring within 10 s after the application of the test solution. It should be noted that there is a clear correlation between the bacterial concentration and the intensity of the red inner ring (Figure 6a). The red inner ring is originated from the immuno-4GS@AuNPs bound

DOI: 10.1021/acsami.9b16075
ACS Appl. Mater. Interfaces 2019, 11, 46472−46478

to the surface of the target bacteria, which were too large to migrate through the NCM, thus its intensity should be proportional to the concentration of the target bacteria. The detection sensitivity of RFCI toward the target bacteria was determined to be 10^3 CFU/mL in buffered solution (PBS). Furthermore, the specificity of RFCI was tested using a sample containing 10^5 CFU/mL of nontarget bacteria, *Bacillus cereus* (B), *Staphylococcus aureus* (S), and *Vibrio cholerae* (V). The presence of high concentration of a nontarget bacteria in the test sample did not contribute to the formation of the red inner ring because the immuno-4GS@AuNPs are specific only to the target bacteria (Figure 6a). The results showed that none of the test samples except the one containing the target bacteria, *E. coli* O157:H7, formed an inner ring. Furthermore, whole milk intentionally spiked with varying concentrations of *E. coli* O157:H7 was tested to examine the applicability of RFCI to detect target bacteria in a real food matrix. The immuno-4GS@AuNP mixed with whole milk without target bacteria did not form a red inner ring, indicating that the immuno-AuNPs prepared with 4GS bifunctional linker retained its colloidal stability and did not form undesirable aggregation in a sample containing complicated food components, such as fats, proteins, carbohydrates, salts, and so on. The intensity of the inner ring was proportional to the concentration of target bacteria in whole milk. The limit of detection (LOD) of RFCI by naked eyes was found to be 10^3 CFU/mL, which is comparable to its performance in PBS buffer, indicating that antigen-binding affinity of immuno-4GS@AuNPs did not interfere with the presence of milk matrices. On the other hand, the LOD of RFCI with immuno-AuNPs prepared by pH-mediated adsorption of antibodies was found to be 10^4 CFU/mL, which is an order of magnitude higher than that of immuno-4GS@AuNPs (Figure S7). The number of target bacteria in the test sample was further quantified using an image analysis program. The intensities of the red inner ring, reflecting the concentration of target bacteria, were analyzed by flatbed scanning and gray value (Figure 6b). The ratio of the gray value in the inner ring (G_I) to the total gray value in the radial pattern was plotted as a function of the concentration of *E. coli* O157:H7 (Figure 6c). The ratio of the intensity was well fitted with the concentration of target bacteria in the milk sample, showing the potential of this system for quantitative analysis of target pathogenic bacteria in food samples. The slightly lower signal intensity in whole milk in comparison to the buffered condition might be attributed to the interference of milk components. However, the colorimetric sensing system with such a low LOD in real food samples without any pretreatment would be a meaningful step toward the development of a sensitive on-site detection system to monitor the safety of food. In addition, the sensitivity of this RFCI detection system could be further improved by employing an appropriate pretreatment, such as concentration of target bacteria from a large volume of sample using the magnetic separation technique.

CONCLUSIONS

In this study, we demonstrated that the colloidal stability of chromatic immuno-AuNPs and the immobilization efficiency of antibodies onto the AuNPs were significantly improved by employing quadruply repeated gold-binding peptides-tagged staphylococcal protein G (4GS) as a bifunctional linker for oriented immobilization of antibodies. In particular, the chronic problem associated with the salt-induced aggregation of AuNPs was resolved by introducing the linker protein on the surface of AuNPs, whose colloidal stability was maintained in the presence of NaCl up to 500 mM. The colloidal stability of the chromatic agent is critical when applied to the paper-based immunoassay because the aggregation of AuNPs caused by any salts in the sample would hinder the free flow of chromatic agents and eventually impair the performance of the detection system. The concentration of immobilized antibodies on the surface of AuNPs with the bifunctional linker protein was about half of that prepared by pH-mediated adsorption. However, the specific binding capacity of the immuno-4GS@AuNPs prepared with the linker protein toward target bacteria was significantly higher than that prepared by the conventional method. We applied the developed immuno-4GS@AuNPs to a paper-based RFCI for the detection of pathogenic bacteria in milk. RFCI is advantageous for the detection of large analytes, such as microorganisms, because the low mobility of microorganisms through the NCM is the key parameter of this system, whereas such characteristics negatively affect the performance of conventional lateral flow immunoassay. The enhanced colloidal stability of the immuno-4GS@AuNPs together with its excellent binding capacity toward target bacteria enabled us to detect *E. coli* O157:H7 as low as 10^3 CFU/mL in whole milk in 10 min. The RFCI results could also be converted into a grayscale value by simple image processing for quantitative determination of target pathogenic bacteria. The developed paper-based diagnostic tool would provide a simple, cost-effective, and sensitive means of detecting the presence of bacteria in samples containing complicated food matrices.

ASSOCIATED CONTENT

Supporting Information

The Supporting Information is available free of charge at https://pubs.acs.org/doi/10.1021/acsami.9b16075.

Experimental details of chemicals, construction, DNA sequence, expression, and purification of 4GS linker protein; map of expression vector harboring 4GBP/SPG gene; sodium dodecyl sulfate-polyacrylamide gel electrophoresis analysis of purified proteins; TEM image and histogram of particle size distribution of 4GS@AuNPs; surface charge of AuNPs and 4GS@AuNPs; amount of 1GS and 4GS bound to the same concentration of AuNPs; UV−visible spectra of AuNPs treated with or without 100 mM NaCl; and RFCI for detecting *E. coil* O157:H7 in whole milk by using the immuno-AuNPs that were prepared by physical adsorption of antibody onto the AuNPs (PDF)

AUTHOR INFORMATION

Corresponding Author

*E-mail: youngkim@khu.ac.kr. Phone: +82-31-201-3830.

ORCID

Young-Rok Kim: 0000-0001-6448-6079

Author Contributions

Y.-R.K., K.L., and I.-H.S. designed the study. K.L., J.R., I.-H.S., K.-B.J., and S.-M.Y. performed experiments on the synthesis and characterization of materials and development of analytical method based on the radial chromatography. Y.-R.K. and K.L. wrote the manuscript.

DOI: 10.1021/acsami.9b16075
ACS Appl. Mater. Interfaces 2019, 11, 46472−46478

Notes

The authors declare no competing financial interest.

■ ACKNOWLEDGMENTS

This research was carried out with the support of Cooperative Research Program for Agriculture Science and Technology Development (project no. PJ01423803), Rural Development Administration, Republic of Korea.

■ REFERENCES

(1) Luo, K.; Kim, H.-Y.; Oh, M.-H.; Kim, Y.-R. Paper-based Lateral Flow Strip Assay for the Detection of Foodborne Pathogens: Principles, Applications, Technological Challenges and Opportunities. *Crit. Rev. Food Sci. Nutr.* **2018**, *47*, 1−14.

(2) Luo, K.; Jeong, K.-B.; You, S.-M.; Lee, D.-H.; Jung, J.-Y.; Kim, Y.-R. Surface-Engineered Starch Magnetic Microparticles for Highly Effective Separation of a Broad Range of Bacteria. *ACS Sustainable Chem. Eng.* **2018**, *6*, 13524−13531.

(3) Park, J.; Shin, J. H.; Park, J.-K. Pressed Paper-Based Dipstick for Detection of Foodborne Pathogens with Multistep Reactions. *Anal. Chem.* **2016**, *88*, 3781−3788.

(4) Kong, M.; Shin, J. H.; Heu, S.; Park, J.-K.; Ryu, S. Lateral Flow Assay-based Bacterial Detection Using Engineered Cell Wall Binding Domains of a Phage Endolysin. *Biosens. Bioelectron.* **2017**, *96*, 173−177.

(5) Park, B. H.; Oh, S. J.; Jung, J. H.; Choi, G.; Seo, J. H.; Kim, D. H.; Lee, E. Y.; Seo, T. S. An Integrated Rotary Microfluidic System with Dna Extraction, Loop-Mediated Isothermal Amplification, and Lateral Flow Strip based Detection for Point-of-Care Pathogen Diagnostics. *Biosens. Bioelectron.* **2017**, *91*, 334−340.

(6) Parolo, C.; de la Escosura-Muñiz, A.; Merkoçi, A. Enhanced Lateral Flow Immunoassay Using Gold Nanoparticles Loaded with Enzymes. *Biosens. Bioelectron.* **2013**, *40*, 412−416.

(7) Marathe, S. A.; Chowdhury, R.; Bhattacharya, R.; Nagarajan, A. G.; Chakravortty, D. Direct Detection of Salmonella without Pre-Enrichment in Milk, Ice-cream and Fruit Juice by PCR against hilA Gene. *Food Control* **2012**, *23*, 559−563.

(8) Cui, M.; Liu, R.; Deng, Z.; Ge, G.; Liu, Y.; Xie, L. Quantitative Study of Protein Coronas on Gold Nanoparticles with Different Surface Modifications. *Nano Res.* **2014**, *7*, 345−352.

(9) Kumar, S.; Aaron, J.; Sokolov, K. Directional Conjugation of Antibodies to Nanoparticles for Synthesis of Multiplexed Optical Contrast Agents with both Delivery and Targeting Moieties. *Nat. Protoc.* **2008**, *3*, 314.

(10) Saha, B.; Evers, T. H.; Prins, M. W. J. How Antibody Surface Coverage on Nanoparticles Determines the Activity and Kinetics of Antigen Capturing for Biosensing. *Anal. Chem.* **2014**, *86*, 8158−8166.

(11) Ko, S.; Park, T. J.; Kim, H.-S.; Kim, J.-H.; Cho, Y.-J. Directed Self-assembly of Gold Binding Polypeptide-Protein A Fusion Proteins for Development of Gold Nanoparticle-based SPR Immunosensors. *Biosens. Bioelectron.* **2009**, *24*, 2592−2597.

(12) Luo, K.; Park, K.-H.; Lee, D.-H.; Hong, C.-E.; Song, Y.-W.; Yoo, S.-H.; Kim, Y.-R. Self-assembly Kinetics of Debranched Short-Chain Glucans from Waxy Maize Starch to Form Spherical Microparticles and its Applications. *Colloids Surf., B* **2019**, *176*, 352−359.

(13) Luo, K.; Jeong, K.-B.; You, S.-M.; Lee, D.-H.; Kim, Y.-R. Molecular Rearrangement of Glucans from Natural Starch to Form Size-Controlled Functional Magnetic Polymer Beads. *J. Agric. Food Chem.* **2018**, *66*, 6806−6813.

(14) Luo, K.; Jeong, K.-B.; Park, C.-S.; Kim, Y.-R. Biosynthesis of Superparamagnetic Polymer Microbeads via Simple Precipitation of Enzymatically Synthesized Short-Chain Amylose. *Carbohydr. Polym.* **2018**, *181*, 818−824.

(15) Lee, J. M.; Park, H. K.; Jung, Y.; Kim, J. K.; Jung, S. O.; Chung, B. H. Direct Immobilization of Protein G Variants with Various Numbers of Cysteine Residues on a Gold Surface. *Anal. Chem.* **2007**, *79*, 2680−2687.

(16) So, C. R.; Tamerler, C.; Sarikaya, M. Adsorption, Diffusion, and Self-Assembly of an Engineered Gold-Binding Peptide on Au(111) Investigated by Atomic Force Microscopy. *Angew. Chem., Int. Ed.* **2009**, *48*, 5174−5177.

(17) So, C. R.; Kulp, J. L.; Oren, E. E.; Zareie, H.; Tamerler, C.; Evans, J. S.; Sarikaya, M. Molecular Recognition and Supramolecular Self-Assembly of a Genetically Engineered Gold Binding Peptide on Au{111}. *ACS Nano* **2009**, *3*, 1525−1531.

(18) Luo, K.; Lee, D.-H.; Adra, H. J.; Kim, Y.-R. Synthesis of Monodisperse Starch Microparticles through Molecular Rearrangement of Short-Chain Glucans from Natural Waxy Maize Starch. *Carbohydr. Polym.* **2019**, *218*, 261−268.

(19) Ghodbane, S.; Ballutaud, D.; Omnès, F.; Agnès, C. Comparison of the XPS Spectra from Homoepitaxial {111}, {100} and Polycrystalline Boron-Doped Diamond Films. *Diamond Relat. Mater.* **2010**, *19*, 630−636.

(20) Zhao, X.; Pan, F.; Cowsill, B.; Lu, J. R.; Garcia-Gancedo, L.; Flewitt, A. J.; Ashley, G. M.; Luo, J. Interfacial Immobilization of Monoclonal Antibody and Detection of Human Prostate-Specific Antigen. *Langmuir* **2011**, *27*, 7654−7662.

DOI: 10.1021/acsami.9b16075
ACS Appl. Mater. Interfaces 2019, 11, 46472−46478